Superior Cycling Performance of a Novel NKVO@Polypyrrole Composite Anode for Aqueous Rechargeable Lithium-Ion Batteries

Najeeb ur Rehman Lashari[a], Mingshu Zhao*[a], Qingyang Zheng[b], Wenyuan Duan[a], Xiaoping Song[a]

(1. School of Science, Key Laboratory of Shaanxi for Advanced Functional Materials and Mesoscopic Physics, MOE Key Laboratory for Nonequilibrium Synthesis and Modulation of Condensed Matter, Xi'an Jiaotong University, Xi'an, 710049, Shaanxi, China; 2. Xi'an High Tech Res Inst, Xi'an 710025, Shaanxi, China.)

(Supporting information)

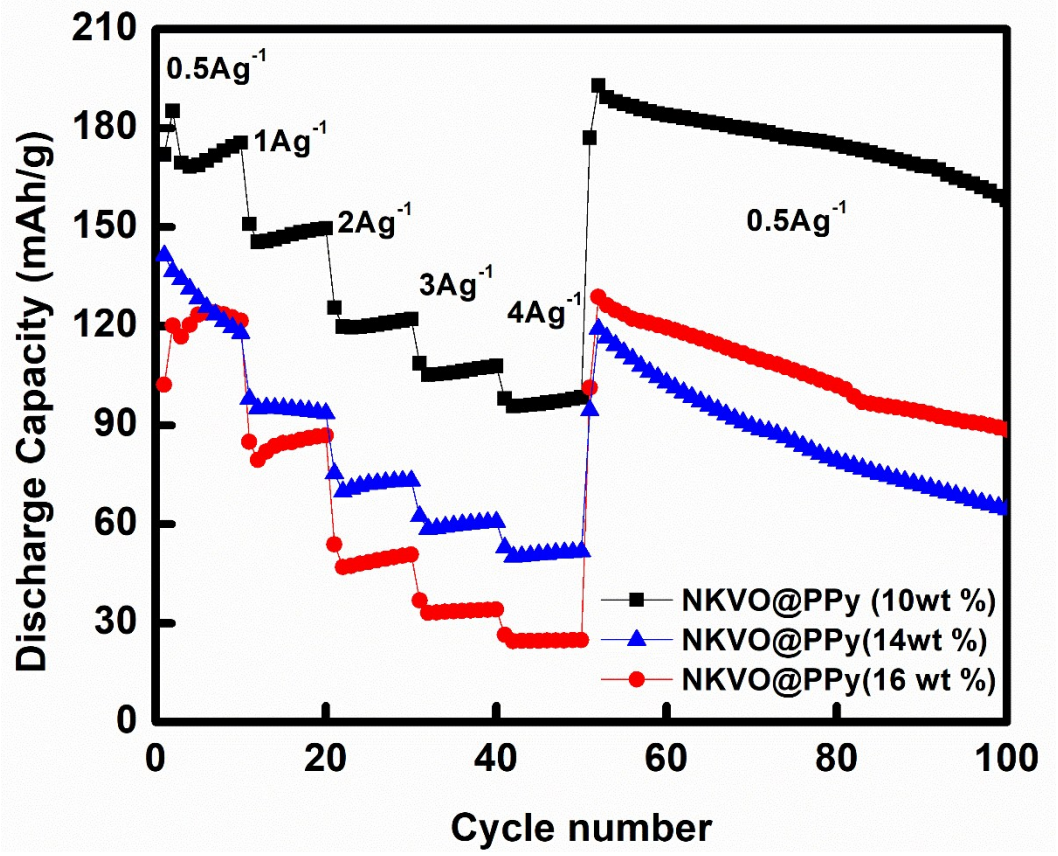

Figure 1S show the discharge performance of different weight % coated compound NKVO@PPy at current rates of 0.5, 1, 2, 3 and 4Ag^{-1} respectively.

“Figure 1S show the rate performance of NKVO@PPy compound with different weight percentage of PPy content, a clear decrease in terms of discharge capacity is observed as PPy content increase. That same effect has been reported by Gao et. al.[1]”

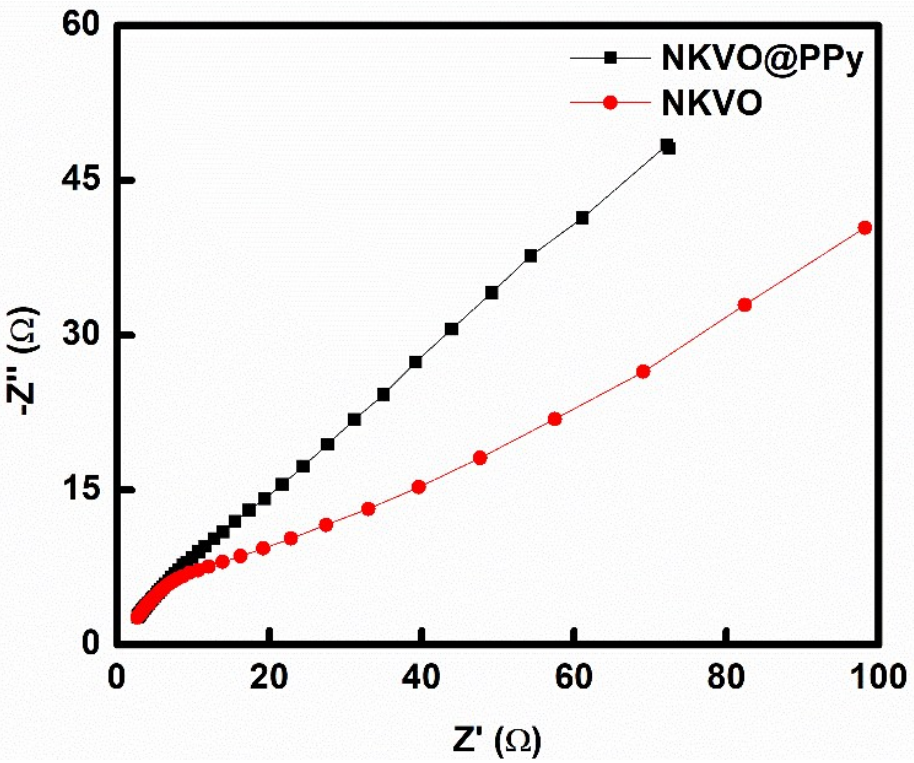

Figure 2S EIS Nyquist patterns of NKVO in red and NKVO@PPy in black.

Figure 2S shows the EIS plot of pristine and PPy coated NKVO, Nyquist patterns are composed of a high-frequency arc and low-frequency inclined line, which corresponded with the charge transfer resistance of the electrode reaction and Warburg resistance of the lithium-ion from the electrolyte interface to the inner of electrode materials, respectively. As it can be seen from the curve that low frequency arch for NKVO@PPy becomes shallower suggest reduction in charge transfer resistance as compared to pristine NKVO. The decrease in transfer resistance for NVO@PPy in the ARLB was probably caused by an increase in Li^+ conductivity with lithium-ion insertion.

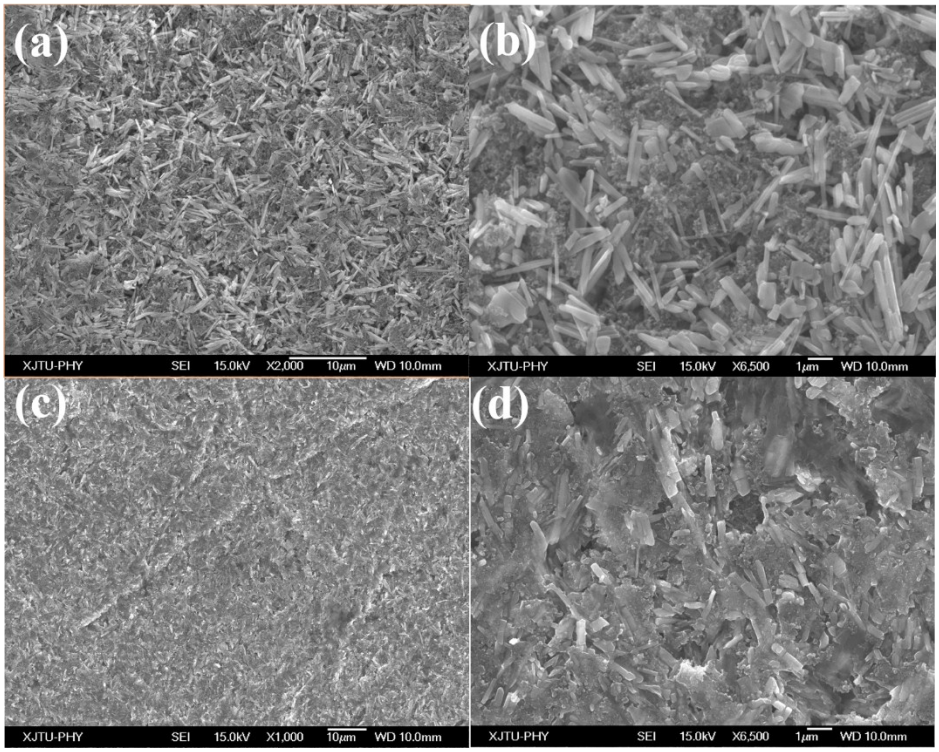

Figure 3S Shows the SEM images of NKVO@PPy coated on Nickel mesh (a) and (b) before cycling, (c) and (d) after 400cycles of charge/discharge at $4Ag^{-1}$.

SEM and XRD measurements for cycled NKVO@PPy anode were carried out in order to further confirm the cycling stability of the anode. As shown in Figure. 3S (a) and (b), except for a bit of carbon, the microrods of NKVO@PPy material was were attached. Figure 3S (c) and (d) shows the morphologies after 400 cycles of NKVO@PPy anode at $4Ag^{-1}$. After long-term cycling, the surface of electrode becomes rough and shows obvious large and disappearance of microrods, indicating the generation of byproducts.

Table 1S Provides overview of PPy modified coated anode materials for ARLB in comparison of our work

ARLB system	**Initial CAPACITY; $mAhg^{-1}$ (current rate; Ag^{-1})**	**Final Capacity $mAhg^{-1}$ (cycle Number)**	**Reten-tion Rate**	**Ref**
MoO_3@PPy//$LiMn_2O_4$	110 (0.5)	100 (150)	90%	[2]
LiV_3O_8@PPy//AC	95 (0.25)	81 (10)	84%	[3]
S@PPy	163 (0.1)	137 (100)	84%	[4]
V_2O_5@PPy//$LiMn_2O_4$	95.2 (0.1)	81.5 (100)	85%	[5]
MWCNTs@S@PPy//$LiMn_2O_4$	120 (0.5)	109 (120)	91%	[6]
NKVO@PPy//$LiMn_2O_4$	115 (4)	64.5 (400)	55%	Our work

Added References

1. X. W. Gao, Y. F. Deng, D. Wexler, G. H. Chen, S. L. Chou, H. K. Liu, Z. C. Shi and J. Z. Wang, *Journal of Materials Chemistry A*, 2015, **3**, 404-411.
2. W. Tang, L. Liu, Y. Zhu, H. Sun, Y. Wu and K. Zhu, *Energy & Environmental Science*, 2012, **5**, 6909-6913.
3. L. L. Liu, X. J. Wang, Y. S. Zhu, C. L. Hu, Y. P. Wu and R. Holze, *Journal of Power Sources*, 2013, **224**, 290-294.
4. J. Shao, X. Li, L. Zhang, Q. Qu and H. Zheng, *Nanoscale*, 2013, **5**, 1460-1464.
5. C. Liang, D. Fang, Y. Cao, G. Li, Z. Luo, Q. Zhou, C. Xiong and W. Xu, *Journal of Colloid and Interface Science*, 2015, **439**, 69-75.
6. W. Tang, X. Gao, Y. Zhu, Y. Yue, Y. Shi, Y. Wu and K. Zhu, *Journal of Materials Chemistry*, 2012, **22**, 20143-20145.